This document is the accepted manuscript version of the following article:
Bakkour, R., Bolotin, J., Sellergren, B., & Hofstetter, T. B. (2018). Molecularly imprinted polymers for compound-specific isotope analysis of polar organic micropollutants in aquatic environments. Analytical Chemistry, 90(12), 7292-7301. https://doi.org/10.1021/acs.analchem.8b00493

# Molecularly-imprinted polymers for compound-specific isotope analysis of polar organic micropollutants in aquatic environments

Rani Bakkour,[†,‡,¶] Jakov Bolotin,[†] Börje Sellergren,[§] and Thomas B. Hofstetter[*,†,‡]

*Eawag, Swiss Federal Institute of Aquatic Science and Technology, Dübendorf, Switzerland, Institute of Biogeochemistry and Pollutant Dynamics, ETH Zürich, Zürich, Switzerland, , and Department of Biomedical Sciences, Malmö University, Malmö, Sweden*

E-mail: thomas.hofstetter@eawag.ch

[*]To whom correspondence should be addressed
[†]Eawag
[‡]ETH Zürich
[¶]present address: Technical University of Munich, Chair for Analytical Chemistry and Water Chemistry, München, Germany
[§]Malmö University

## Abstract

Compound-specific isotope analysis (CSIA) of polar organic micropollutants in environmental waters requires a processing of large sample volumes to obtain the required analyte masses for analysis by gas chromatography / isotope-ratio mass spectrometry (GC/IRMS). However, the accumulation of organic matter of unknown isotopic composition in standard enrichment procedures currently compromises the accurate determination of isotope ratios. We explored the use of molecularly-imprinted polymers (MIPs) for selective analyte enrichment for $^{13}C/^{12}C$ and $^{15}N/^{14}N$ ratio measurements by GC/IRMS using 1*H*-benzotriazole, a typical corrosion inhibitor in dishwashing detergents, as example of a widely detected polar organic micropollutant. We developed procedures for the treatment of $>$ 10 L of water samples, in which custom-made MIPs enabled the selective cleanup of enriched analytes in organic solvents obtained through conventional solid phase extractions. Hydrogen bonding interactions between the traziole moiety of 1*H*-benzotriazole and the MIP were responsible for selective interactions through an assessment of interaction enthalpies and $^{15}N$ isotope effects. The procedure was applied successfully without causing isotope fractionation to river water samples as well as in- and effluents of wastewater treatment plants containing $\mu$g/L concentrations of 1*H*-benzotriazole and dissolved organic carbon (DOC) loads of up to 28 mg C/L. MIP-based treatments offer new perspectives for CSIA of organic micropollutants through the reduction of the DOC-to-micropollutant ratios.

# Introduction

The analysis of stable isotope ratios in organic soil and water contaminants has become a widely used approach to identify the sources of pollution and to identify (bio)degradation pathways.[1–7] Whereas constant ratios of $^{13}C/^{12}C$, $^{2}H/^{1}H$, $^{15}N/^{14}N$, and of other elements in a compound enable one to infer precursor materials, synthesis routes, and formation pathways of pollutants,[8–14] changes of isotope ratios lead to stable isotope fractionation patterns that reveal the (bio)chemical reaction by which a pollutant is degraded.[15–21] However, due to the poor sensitivity of gas and liquid chromatography used in combination with isotope-ratio mass spectrometry,[22–25] the applications of compound-specific isotope analysis (CSIA) have largely focused on so-called legacy contaminants such as halogenated solvents, nitroaromatic explosives, and fuel constituents[26–33] Those compounds are often found in the high $\mu$g $L^{-1}$ to mg $L^{-1}$ concentration range and can be extracted from the environmental matrices in straightforward procedures, for example, through transfer of the analytes into the gas phase and enrichment onto solid sorbents.[32–37] Unfortunately, such procedures are not necessarily applicable for CSIA of polar organic micropollutants of current interest[38] such as pesticides, pharmaceuticals, consumer chemicals, and personal care products. Their sub-$\mu$g $L^{-1}$ concentrations in natural and treated waters require the processing of large sample volumes greater than 5 L by solid-phase extractions (SPE, e.g.,[39]) to obtain the necessary analyte mass for isotope-ratio mass spectrometry. Moreover, the inherently poor selectivity of SPE-based procedures will very likely lead to a co-enrichment of organic matter of unknown isotopic composition and thus compromise accurate isotope ratio measurements.

One promising option to increase the selectivity of analyte enrichment procedures is the use of molecularly-imprinted polymers (MIPs). MIPs are synthetic, typically custom-made materials capable of molecular recognition of a target analyte through specific intermolecular interactions.[40–44] Synthesis is carried out in the presence of the target analyte and involves the polymerization of functional monomers that are selected based on their ability to interact with functional groups of the target molecule. Therefore, the final materials exhibit a three-dimensional structure with high specificity.[45] Even though the concept of solid-phase extraction with molecularly-imprinted

polymers (MISPE) has been used successfully for years,[40,46–48] it has never been applied in combination with isotopic analyses. In fact, MISPE based on non-covalent interaction between analyte and sorbent seems ideally suited for the treatment of SPE-extracts, in which polar organic micropollutants are normally enriched from large volumes of water samples.[49] Only $\mu$L volumes of organic solvents can be injected onto gas chromatographs coupled to isotope-ratio mass spectrometers. The substantial analyte enrichment to the mg $L^{-1}$ level causes concomitant enrichment of organic matrix and, therefore, requires further sample treatment. Because those extracts typically consist of organic solvents, polar organic micropollutants can be extracted based on H-bonding and ionic interactions with the MIP without interferences of water.

The goal of this work was to explore new sample clean-up strategies based on molecularly-imprinted polymers for the stable isotope analysis of polar organic micropollutants in aquatic environments. Here, we focused our work on the analysis of $^{13}C/^{12}C$ and $^{15}N/^{14}N$ ratios of 1*H*-benzotriazole (1*H*-BT), a corrosion inhibitor, which is widely used in dishwashing detergents. Like many polar organic micropollutants, 1*H*-BT is too persistent to be degraded in waste water treatment plants (WWTP) and therefore found in $\mu$g $L^{-1}$ concentrations in rivers as well as influents and effluents of WWTPs containing very different organic matrices.[50–52] The specific objectives of our work were to (i) propose sample treatment procedures for MISPE-based stable isotope analysis through the synthesis and application of a custom-made MIP for 1*H*-BT. (ii) We characterized the selectivity of our materials in a comparison with other polar organic micropollutants such as triazines and substituted benzotriazoles and (iii) evaluated the potential of method-induced isotope fractionation from incomplete analyte recovery. (iv) Finally, we illustrate how MISPE-based procedures for CSIA can be applied in different matrices by analysing $\delta^{13}C$ and $\delta^{15}N$ of 1*H*-BT in riverwater, influent and effluent of a WWTPs, as well as in dishwashing detergent taps.

# Experimental section

A list of all chemicals including suppliers and purities is provided in the Supporting Information (SI).

## Safety considerations

Milling and sieving the synthesized polymers can generate dust. The processing of materials should be carried out under the fumehood. Additionally, gloves, goggles and respiration mask are advised to be worn. The radical generator, azobisisobutyronitrile, decompose at temperature $\geq$ 45 °C and may explode if large amounts are exposed to high temperatures. Do not exceed temperature of 40 °C during its purification.

## Synthesis of molecularly-imprinted polymers

Molecularly-imprinted polymers were synthesized following an adapted procedure of Chapuis et al.[53] for terbutylazine. The polymerization mixture consisted of 119.1 mg (1 mmol) 1H-benzotriazole (1*H*-BT) as template, 344.4 mg (4 mmol) methacrylic acid as a functional monomer, 3964 mg (20 mmol) ethylene glycol dimethacrylate as crosslinker, 39.4 mg (0.24 mmol) azobisisobutyronitrile as radical generator, and 5.6 mL dichloromethane as porogene. We dissolved the template in the functional monomer, cooled the solution to 0℃ for 15 minutes and added the remaining reagents. The polymerization mixture was purged with $N_2$ in a borosilicate glass tube (OD = 18 mm, ID = 15 mm), sealed with a screw-cap, and placed in an ice bath for 30 minutes. The same procedure was used for preparation of non-imprinted polymer (NIP) except for the absence of the template 1*H*-BT.

Polymerization took place over 24 hours at 2 ± 0.2℃ by immersing the glass tubes in a merry-go-round photoreactor (DEMA 125, Hans Mangels GmbH, Bornheim-Roisdorf, Germany; Figure S1) filled with a sodium nitrate filter solution (0.15 M, cut-off of wavelength > 320 nm) and centred with a medium pressure mercury lamp (150 W) surrounded by a borosilicate glass jacket.[54]

After polymerization, the tubes were removed and crushed to recover the polymer monoliths. The polymers were sequentially ground (Mixer Mill MM 301, Retsch GmbH, Germany) and sieved through 100 $\mu$m sieve (Retsch GmbH, Germany). The particle fraction < 100$\mu$m was sedimented in methanol to obtain particle size distribution between 20 and 100 $\mu$m. We removed the template by ten repetitive cycles of Soxhlet extraction using mixtures of methanol and formic acid (90/10 vol-%) until ≥ 98% of the 1*H*-benzotriazole was recovered. Nonimprinted polymers were extrated in the identical manner. The identical procedure was applied to synthesize a MIP with 5-,6-$(CH_3)_2$-benzotriazole as template for the quantitative analysis of imprinting efficiency. Possible interferences of residual analytes on the accuracy of stable isotope analysis were evaluated exemplarily for 1*H*-BT through (a) quantification of its concentration before and after the use of MIPs with 1*H*-BT in organic solvent and (b) the comparison of $^{13}C/^{12}C$ and $^{15}N/^{14}N$ ratios of 1*H*-BT before and after the use of MIPs with 1*H*-BT spiked river water samples.

## Sample preparation procedures using molecularly-imprinted polymers

The multi-step procedure for the enrichment and purification of 1*H*-BT in (a) in- an effluent of waste water treatment plants (WWTP), (b) spiked river water, and (c) dishwashing tabs is shown schematically in Figure 1. Generally, sample preparation consisted of two solid phase extraction steps (Fig. 1, **B** and **D**) with different pre- and post treatments.

### Enrichment of 1*H*-BT from waste water plant influent and effluent

Samples from WWTP influent (5 L, sample no. **1** in Figure 1, step **A**) and effluent (10 L) were filtered through 0.7 $\mu$m glass fiber filters (Whatman, GF/F 47mm) and acidified with HCl (32 %) to pH 2.0. Filtered samples **2** containing 1*H*-BT were enriched by conventional solid phase extraction using OASIS HLB cartridges (Waters, 6 g, 35 mL) in step **B** using a 12-port vacuum extraction manifold (Supelco, Switzerland). Prior to sample loading, cartridges were conditioned with 100 mL hexane, 100 mL ethyl acetate, 100 mL methanol and 100 mL MiliQ water. Water samples **2** were percolated through the cartridges using a vacuum pump at a flow rate of ≤ 7.2 mL/min

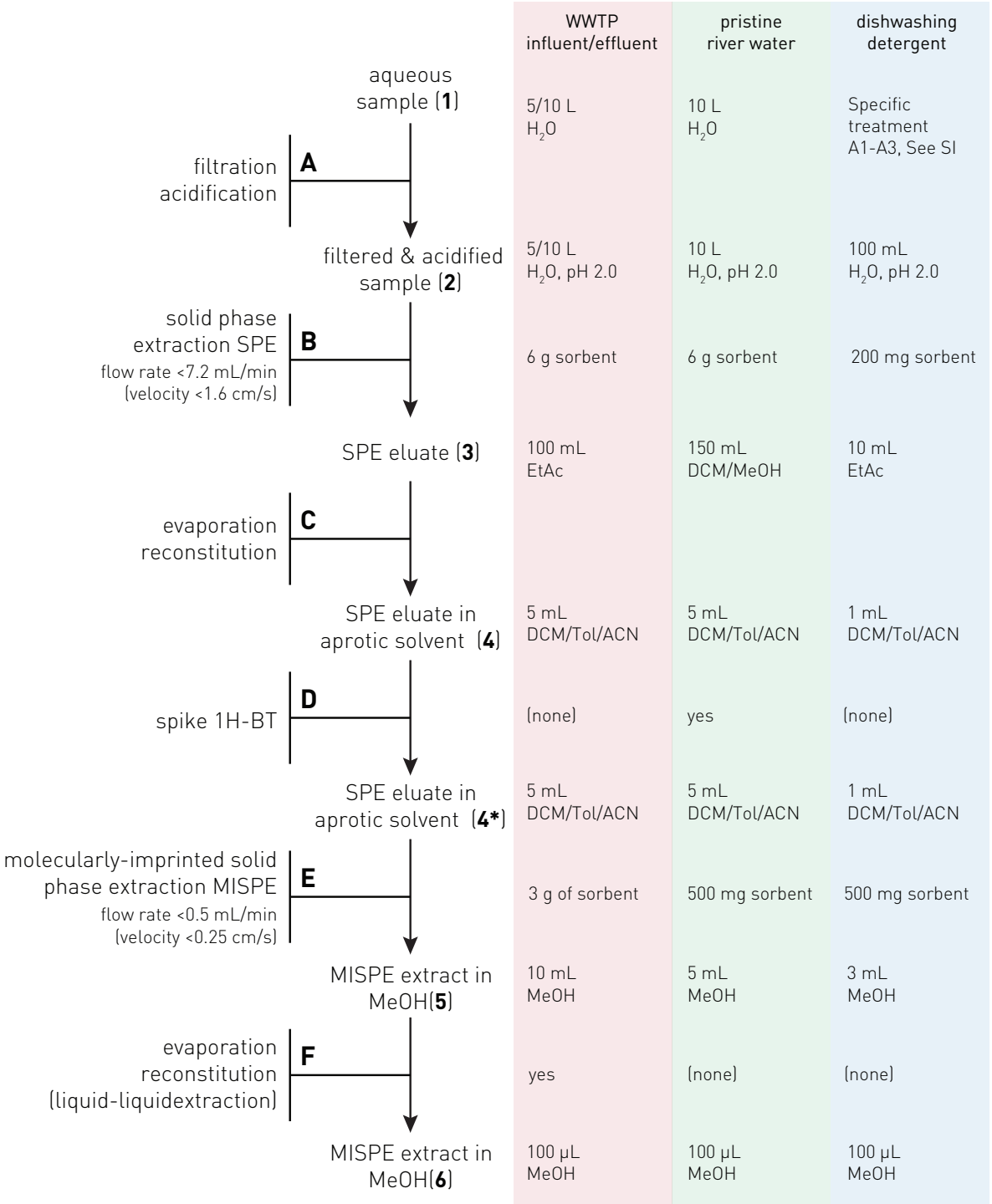


**Figure 1.** Sample preparation procedure for analysis of $1H$-benzotriazole ($1H$-BT) optimized for different water matrices (influent and effluent of waste water treatment plants (WWTP), spiked river water, and dishwashing detergents. Capital letters **A** to **F** stand for treatment steps, bold numbers **1** to **6** refer to samples obtained throughout the treatment sequence. Acronyms of organic solvents stand for acetonitrile (ACN), ethylacetate (EtAc), dichloromethane (DCM), methanol (MeOH), and toluene (Tol). Details on the specific initial processing steps of solid, gel-like, and liquid dishwashing detergents are shown in Figure S2.

corresponding to a linear velocity of ≤ 1.6 cm/s. Subsequently, the cartridges were dried under vacuum overnight and eluted in 100 mL of ethylacetate. In step **C**, the SPE eluates **3** were dried using rotary evaporator (Büchi, Switzerland) at 40 °C under a gentle stream of $N_2$. Dry residues were reconstituted in 5 mL of aprotic organic solvent (**4**), that is a dichloromethane/toluene/acetonitrile mixture (55/40/5 vol %) for molecularly-imprinted solid-phase extraction (MISPE, step **E**).

For 5 mL of sample **4**, 3 g of the 1*H*-BT-imprinted polymer sorbent was packed in PP tubes (12 mL) and conditioned with 50 mL of methanol/formic acid (90/10 vol %), 50 mL of methanol, and 50 mL of dichloromethane/toluene/acetonitrile (55/40/5 vol%). Following sample percolation, the sorbent was washed with 40 mL of dichloromethane/toluene/acetonitrile (55/40/5 vol%). Thereafter, the sorbed analytes were eluted with 10 mL methanol. Throughout the sample percolation, wash, and elution step, the flow rate did not exceed 0.5 mL/min or 0.25 cm/s. In step **F**, the MISPE eluate **5** was evaporated under a stream of $N_2$ and reconstituted in 1 mL of methanol, followed by a solvent-solvent extraction with *n*-hexane to reduce interferences of the organic matrix further (see discussion in conclusion section). The methanol extract was extracted five times with 1 mL *n*-hexane for each extraction step. The *n*-hexane extracts (5 mL) were evaporated again and reconstituted in methanol to obtain target analyte concentrations within the linear range of the isotope-ratio mass spectrometer.

### Cleanup of 1*H*-BT from spiked river water

Enrichment of 1*H*-BT from 10 L of river water of the analyte followed the same procedure described above with some minor modifications (Figure 1). In step **B**, the cartridge was eluted with 150 mL of dichloromethane/methanol (97/3 vol %). In step **C**, the sample was evaporated and reconstituted in 5 mL dichloromethane/toluene/acetonitrile (55/40/5 vol %). Thereafter, step **D**, 50 $\mu$L of a 100 mM solution of 1*H*-BT were spiked to SPE eluate **4**. The 1*H*-BT concentration in **4**$^*$ corresponded to a hypothetical riverwater concentration of 6.0 $\mu$g/L. The 5 mL of **4**$^*$ was purified with MISPE (step **E**), for which 500 mg of polymer was packed in PP tubes (6 mL), conditioned as described above and used with a flow rate of ≤ 0.3 ml/min or ≤ 0.25 cm/s. The MISPE eluate **5** was evaproated

under a stream of $N_2$ in step **F** to 100 $\mu$L without a liquid-liquid extraction step.

### Enrichment of 1*H*-BT from dishwashing detergent

Samples from different dishwashing detergents required additional pre-treatment prior to SPE as illustrated in Figure 1, steps **A1** to **A3**. Detergent tabs were crushed with a pestle and mortar and dried in the oven at 40 °C overnight as were powder detergents. The crushed tabs and powders were then milled and homogenized in a ball mill with a frequency of 30 Hz for 2 mins (**A1**). 100 mg of the homogenized detergent powder or unprocessed liquids and gels (**1b**) were dissolved in 100 mL water and ultra-sonicated for 15 min in step **A2**. The detergent suspension **1c** was acidified in step **A3** to pH 2.0 using 6 M HCl leading to an acidified detergent suspension (**2**). The latter was subsequently treated according to the steps outlined in Figure 1.

In step **B**, the acidified detergent suspensions were extracted using SPE on OASIS HLB cartridges (Waters, 200 mg, 6 mL) at flow rates $\leq$ 1.9 mL min$^{-1}$ or $\leq$ 1.6 cm s$^{-1}$. The cartridges were eluted with 10 mL ethyl acetate. In step **C**, evaporation/reconstitution resulted in 1 mL dichloromethane/toluene/acetonitrile (55/40/5 vol%) mixture. Samples **4** were purified using MISPE (step **E**) with 500 mg benzotriazole-imprinted polymer sorbent which was packed in PP tubes (6 mL) and conditioned as described above. After sample percolation, the sorbent was washed with 8 mL of dichloromethane/toluene/acetonitrile (55/40/5 vol %). Elution of 1*H*-BT was carried out with 3 mL methanol. The evaporation/reconstitution (step **F**) yielded 100 $\mu$L of a methanolic solution.

## Sample preparation for isotope fractionation experiments

The extent of C and N isotope fractionation of 1*H*-BT from incomplete recovery during a MISPE procedure (step **E**) was tested in a three-step procedure in the presence and absence of organic matrix from river water samples. (*i*) Two samples containing 100 $\mu$M of 1*H*-BT in 5 mL river water extract in dichloromethane and pristine dichloromethane were loaded onto separate cartridges containing 500 and 100 mg MIP, respectively, while the breakthrough was collected ($F_1$, "load" fraction). Thereafter, (*ii*) the MISPE cartridges were washed with 5 mL dichloromethane leading to

another set of $1H$-BT-containing samples ($F_2$, "wash" fraction). Finally, (*iii*) the remaining $1H$-BT on the MISPE cartridges was eluted using 5 mL methanol ($F_3$, "elute" fraction). The volume of all three fractions were blown down to 100 µL prior to quantification and stable isotope analysis of $1H$-BT.

# Chemical analyses

## Organic compounds in aqueous and organic matrices

Concentrations of benzotriazoles and structurally related compounds (benzothiazoles, triazines) were analyzed by reversed-phase liquid chromatography (Dionex UltiMate 3000 System, Thermofisher) using Supelcosil LC-18 column (250 x 4.6 mm, 5 $\mu$m, Supelco) with isocratic mixtures of water/methanol (70/30 vol%) at a flow rate of 1.0 mL/min. UV-Vis detection was carried out at wavelengths of maximal absorption. Concentrations of these analytes in organic solvents were measured after evaporation to dryness and reconstitution in water/methanol mixtures (70/30 vol%). Samples of 20 $\mu$L were injected from an autosampler cooled to 10°C. Concentrations of benzotriazolesin river water and waste water samples was determined by liquid chromatography coupled to a linear ion trap-Orbitrap high-resolution mass spectrometer (LC/HRMS/MS) in positive mode with electrospray ionization following methods described by Huntscha et al.[52]

## Organic carbon measurements

Dissolved and total organic carbon concentrations (DOC, TOC) were measured using a total organic carbon analyzer (TOC-L, Shimadzu) equipped with a combustion catalytic oxidation unit (680 °C) and a non-dispersive infrared detector. DOC concentrations in river and waste water samples were measured after filtration through a 0.45 $\mu$m filter. TOC concentrations in samples dissolved in organic solvents were determined on the TOC analyzer after evaporation of the solvent under a gentle stream of $N_2$ for 30 min followed by reconstititution of the dry residues in water using ultra-sonication for 15 min and homogenization for 10 min using stand dispersion unit (Polytron

PT 3100, Kinematica).

### Compound-specific isotope analysis

C and N isotope ratio measurements of 1*H*-BT was carried out as described in Spahr et al.[55] by gas chromatography/isotope-ratio mass spectrometry (GC/C/IRMS) using a customized nickel/platinum reactor for analyte combustion at 1000°C. Liquid samples of 1 $\mu$L were injected into a split/ splitless injector coupled to a RTX-5 Amine GC column (30 m × 0.32 mm). Helium was used as carrier gas at constant pressure (100 kPa). The temperature program was 1 min at 80 °C, 15 °C/min to 180 °C (held for 10 min), 40 °C/min to 250 °C (held for 5 min). Isotope ratios are reported as arithmetic means of triplicate measurements with one standard deviation ($\pm\sigma$) as a measure of the uncertainty in the form of isotope signatures ($\delta^{13}$C and $\delta^{15}$N) in per mil (‰) relative to the international reference materials Vienna PeeDee Belemnite ($\delta^{13}C_{VPDB}$) and air ($\delta^{15}N_{air}$). We used a suite of calibrated reference materials with $\delta^{13}$C from −54.6‰ to +7.7‰ and $\delta^{15}$N from −6‰ to +41‰[56,57] as well as repeated measurements of in-house standards (benzotriazoles) in a standard bracketing procedures to ensure accuracy of the measured $\delta^{13}$C and $\delta^{15}$N values.

## Data evaluation

### Selectivity of molecularly-imprinted polymers

The selectivity of MIP and NIP were assessed by high-performance liquid chromatography (HPLC)[45] using a stainless-steel column (53.0 x 3.0 mm, Bischoff, Germany) connected to a pre-column (14 x 3.0 mm). Both pre-column and main column were dry-packed with either MIP or NIP and connected to an HPLC pump. Methanol at a flow rate of 2.0 mL/min was used as eluent to condition and to compress the sorbent in the column. Once a constant back-pressure was maintained in the HPLC system over at least 120 min, the eluent was stopped and the column set was removed leaving the main column for characterization of (a) capacity factors, (b) imprinting factors, and (c) enthalpies of analyte-polymer interaction.

(a) Capacity factors, $k_i$, of benzotriazoles and other organic compounds on the synthesized polymers were determined with eq. 1 using an HPLC system equipped with UV-Vis detector, an autosampler, and a column oven. Chromatographic conditions included acetonitrile as eluent at a constant flow rate of 0.1 mL/min, 50 $\mu$L injection volume of solutions containing the target compounds at concentrations between 5 and 7 mg/L in acetonitrile, UV detection at the corresponding wavelength of maximum absorbance.

$$k_i = \frac{t_i - t_0}{t_0} \tag{1}$$

where $k_i$ is the capacity factor of the analyte $i$ on the synthesized polymer, $t_i$ and $t_0$ are retention times of the analyte and the conservative tracer (acetone), respectively.

(b) Imprinting factors, $IF_i$, are calculated with eq. 2 for each analyte $i$ as the ratio of its capacity factors obtained using the imprinted polymer ($k_{i,\mathrm{MIP}}$) and non-imprinted polymers ($k_{i,\mathrm{NIP}}$), respectively.

$$IF_i = \frac{k_{i,\mathrm{MIP}}}{k_{i,\mathrm{NIP}}} \tag{2}$$

(c) Enthalpies of interaction between the analyte and the synthesized polymers, $\Delta_\mathrm{r}H_i$, were calculated from the slope of van't Hoff equation, eq. 3, where the natural logarithm of capacity factors at three temperatures (278, 288, and 298 K) were plotted versus the corresponding reciprocal absolute temperatures ($1/T$). See section S6 for derivation.

$$\frac{d \ln k_i}{d\,(1/T)} = -\frac{\Delta_\mathrm{r}H_i}{R} \tag{3}$$

where $R$ is the gas constant.

**Isotope fractionation during analyte cleanup with MIP**

The C and N isotope signatures of 1$H$-BT, $\delta^{13}$C and $\delta^{15}$N, in each of the three fractions $F_1$ to $F_3$ of the isotope fractionation experiment were (a) evaluated for the extent of isotope fractionation,

$\Delta^h$E, in case of partial analyte recovery during MISPE cleanup step **E**. (b) With the same data, we quantified an operational N isotope enrichment factor, $\epsilon_N$, for interactions of 1*H*-BT with the MIP during MISPE cleanup step **E**. For such an evaluation, we conceptualized the interaction between 1*H*-BT and the MIP as reactive process during the elution step. The reaction starts with a MISPE cartridge loaded with 1*H*-BT. Analyte molecules eluting in early fractions are considered as having experienced only limited interactions with the polymer. The isotope signatures of 1*H*-BT from these fractions correspond to a small extent of reaction, which we quantify as the fraction that is not longer associated with the MIP, The latter is quantified as $1 - f_{i,\mathrm{MIP}}$, where $f_{i,\mathrm{MIP}}$ is the fraction of 1*H*-BT remaining associated with MIP after an elution step. Consequently, fractions of 1*H*-BT that elute at later stages have undergone more extensive interactions with the MIP and the corresponding 1*H*-BT isotope composition would thus reflect later stages of the reaction.

The extent of C and N isotope fractionation, $\Delta^h$E, was derived based on an isotopic mass balance with eq. 4.

$$\Delta^h\mathrm{E} = \delta^h\mathrm{E}_0 - \sum_{i=1}^{3}\left(m_i \cdot \delta^h\mathrm{E}_i\right) \tag{4}$$

where $\delta^h\mathrm{E}_0$ and $\delta^h\mathrm{E}_i$ are the C and N isotope signatures of 1*H*-BT measured in the stock solution as well as in the three sample fractions $F_i$, and $m_i$ is the mass fraction of 1*H*-BT therein. The operational N isotope enrichment factor, $\epsilon_N$, for the MISPE cleanup step **E** was obtained through non-linear regression of eq. 5.

$$\frac{\delta^{15}\mathrm{N}_{i,\mathrm{MIP}} + 1}{\delta^{15}\mathrm{N}_0 + 1} = (f_{i,\mathrm{MIP}})^{\epsilon_N} \tag{5}$$

where $f_{i,\mathrm{MIP}}$ has the above mentioned meaning. $f_{i,\mathrm{MIP}}$ of the "load" and "wash" fractions ($F_1$ to $F_2$) were calculated with eq. 6. The N isotope signature of 1*H*-BT associated with the MIP after elution step $i$, $\delta^{15}\mathrm{N}_{\mathrm{MIP},i}$, was derived through a mass balance approach as in eq. 7. Note that eq. 7 was applied to calculate $\delta^{15}\mathrm{N}_{i,\mathrm{MIP}}$ for $F_1$ whereas $\delta^{15}\mathrm{N}_{i,\mathrm{MIP}}$ of $F_2$ corresponded to the $\delta^{15}$N-value of 1*H*-BT recovered in the methanolic extract. The N isotope enrichment factor, $\epsilon_N$,

was obtained through non-linear regression of eq. 5 and the corresponding apparent kinetic isotope effect, $^{15}$N-AKIE, from eq. 8 following procedures summarized recently in Pati et al.[58].

$$f_{i,\mathrm{MIP}} = 1 - \sum_{i=1}^{i-1} m_i \tag{6}$$

$$\delta^{15}\mathrm{N}_{i,\mathrm{MIP}} = \frac{\delta^{15}\mathrm{N}_0 - \sum \left(m_i \cdot \delta^{15}\mathrm{N}_i\right)}{1 - \sum m_i} \tag{7}$$

$$^{15}\mathrm{N\text{-}AKIE} = \frac{1}{1 + \epsilon_\mathrm{N}} \tag{8}$$

The deviation of the measured $\delta^{15}$N from the accurate value due to incomplete analyte recovery, $\Delta$, was quantified with a modified form of eq. 5 as in eq. 9.

$$\Delta = \delta^{15}\mathrm{N}_0 - \theta^{\epsilon_\mathrm{N}}(\delta^{15}\mathrm{N}_0 + 1) + 1 \tag{9}$$

where $\Delta$ is the expected deviation of $\delta^{15}$N and $\theta$ is the fractional analyte recovery.

# Results and Discussion

## Isotopic analysis of 1*H*-benzotriazole after selective extraction from spiked river water

We evaluated the applicability of molecularly-imprinted polymers (MIP) for selective analyte cleanup for compound-specific isotope analysis in river water spiked with 1*H*-BT. Figure 2 shows the chromatograms for C isotope ratio measurements of 1*H*-BT for different samples taken at selected treatment procedures steps illustrated in Figure 1. Figure 2a corresponds to the solid-phase extraction eluate **4**$^*$, to which the 1*H*-BT standard was added in an amount that would have corresponded to an aqueous concentration 6.0 $\mu$g/L in the original water sample (**1** in Figure 1). The retention time of 1*H*-BT is indicated with a dashed line and the chromatogram of 1*H*-BT

standard in dichloromethane is shown at the bottom inf Figure 2d. The chromatogram in Figure 2a illustrates that an enrichment of micropollutants from aqueous samples with conventional solid phase extraction procedures (steps **A** to **C**, Figure 1) is concomitant with the accumulation of organic matrix. Because its isotopic composition is not known a priori, background signals from the organic matrix interfere with accurate C isotope ratio measurements by GC/C/IRMS.[5,24,59,60] Qualitative evidence for the selectivity of 1*H*-BT retention on the MIP during sample preparation step **E** was obtained from washing the MIP with dichloromethane/toluene/acetonitrile 55/40/5 vol% (Figure 2b, SPE eluate (**4***) wash). Due to specific interactions of the MIP with 1*H*-BT, the analyte is no longer found in the sample whereas the chromatogram of the organic matrix looks largely identical to the one of the loaded SPE eluate. Finally, the MISPE eluate **5** obtained from washing the polymer with methanol contains primarily 1*H*-BT (green line in Figure 2c). This observation further confirms the selectivity of the synthesized polymer. The excellent recovery of 1*H*-BT in the MISPE eluate **5** of $103 \pm 5\%$ was prerequisite for accurate isotopic analysis. Indeed, the deviation of C and N isotope signatures from its original value $\Delta^{13}$C and $\Delta^{15}$N where $0.5 \pm 0.4‰$ and $0.6 \pm 0.4‰$ and thus within analytical uncertainty of typical measurements by GC/C/IRMS.[5,61] Note that the accuracy of isotopic measurements also rules out possible interferences of residual analytes present on the MIP after synthesis.

## Quantitative evaluation of imprinting efficiency

We assessed the selectivity of 1*H*-BT retention on the MIP by quantifying imprinting factors (*IF*) using eq. 2, the enthalpies of interaction of 1*H*-BT with the MIP ($\Delta H_{\mathrm{MIP}}$), and with the non-imprinted polymer (NIP, $\Delta H_{\mathrm{NIP}}$). Those numbers are compared in Table 1 with a series of structurally related compounds namely, methyl-substituted benzotriazoles (1-$CH_3$-BT, 5-$CH_3$-BT, 5-,6-$(CH_3)_2$-BT), as well as benzothiazole, naphthalene, and atrazine (molecular structures in Figure S3). We observed *IF*-values > 1.0 in acetonitrile, which are indicative of selective binding of the target molecule to the MIP, for 1*H*-BT and the two aromatic ring substituted benzotriazoles, 5-$CH_3$-BT and 5-,6-$(CH_3)_2$-BT. No selectivity, that is $IF \leq 1.0$, were found for other compounds

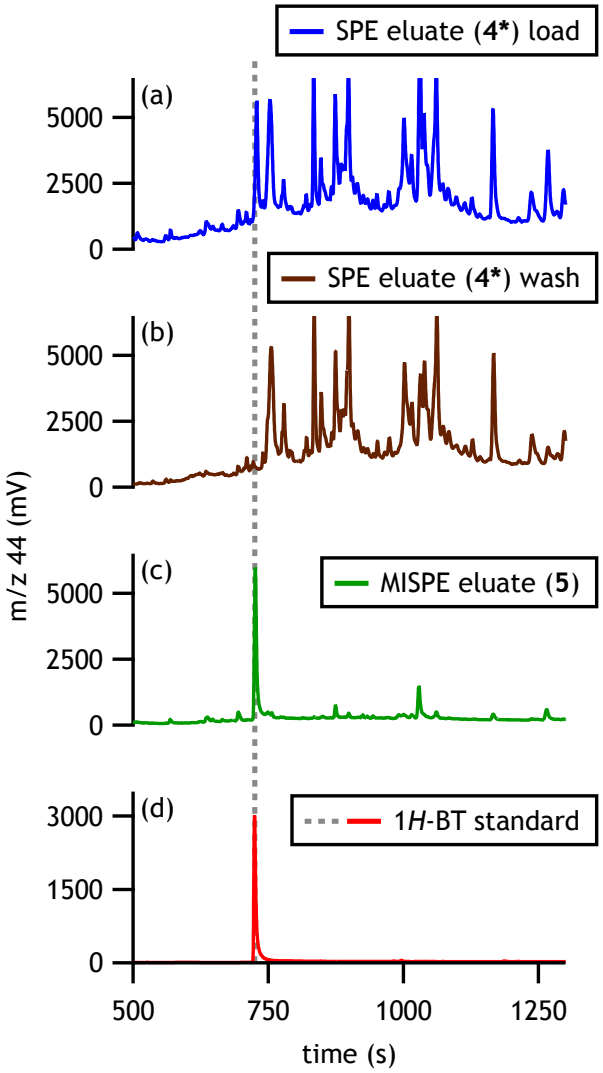


**Figure 2.** Comparison of GC-IRMS chromatograms for C isotope ratio measurement through the operational procedure for cleaning up the SPE eluate of river water spiked with 1*H*-BT (sample **4*** according to Figure 1), (a) SPE eluate **4*** loaded to the MIP, (b) its eluate after washing the MISPE with dichloromethane/toluene/acetonitrile, and, (c) the MISPE extract **5** in methanol, and (d) an 1*H*-BT standard solution.

including *N*-substituted 1-$CH_3$-BT as well as benzothiazole, naphthalene, and atrazine. Note that the magnitude of *IF*-values not only depends on the interactions of analyte and polymer but also on that of the solvent used in the experiments.[62] Whereas the numbers shown in Table 1 may appear small, the precision of *IF*-values of $< 0.1$ (95% confidence intervals) is sufficient for comparisons among different organic analytes here.

**Table 1.** Comparison of imprinting factors (*IF*) and enthalpies of interaction ($\Delta H$) for 1*H*-benzotriazole (1*H*-BT), 5-methyl-1*H*-benzotriazole (5-$CH_3$-BT), 5,6-dimethyl-1*H*-benzotriazole (5-,6-$(CH_3)_2$-BT), 1-methyl-benzotriazole (1-$CH_3$-BT), benzothiazole, naphthalene, and atrazine (structures in Figure S3).

| Parameter | 1*H*-BT | 5-$CH_3$-BT | 5-,6-$(CH_3)_2$-BT | 1-$CH_3$-BT | benzothiazole | napthalene | atrazine |
|---|---|---|---|---|---|---|---|
| *IF* [a] | **1.5** | **1.3** | **1.2** | 1.0 | 0.9 | 0.9 | 1.0 |
| $IF_{(CH_3)_2-BT}$ [b] | 1.1 | 1.3 | 1.6 | 1.0 | n.a. [c] | n.a. | n.a. |
| $\Delta H_{MIP}$ [d,e] | –13.5±0.2 | –12.8±0.4 | –12.2±0.1 | –9.8±0.3 | –10.8±0.1 | –7.1±0.0 | –16.3±0.7 |
| $\Delta H_{NIP}$ [d,e] | –9.5±0.5 | –10.5±0.1 | –10.5±0.2 | –9.5±0.2 | –10.8±0.2 | –7.0±0.1 | -15.8±0.2 |
| $\Delta H_{MIP} - \Delta H_{NIP}$ [d,e] | **–4.0±0.5** [d] | **–2.3±0.4** | **–1.7±0.2** | –0.3±0.3 | 0.0±0.2 | 0.1±0.1 | –0.5±0.8 |

[a] MIP imprinted with 1*H*-BT as template, all values exhibit 95% confidence interval of $\pm \leq 0.1$; [b] MIP imprinted with 5-,6-$(CH_3)_2$-BT as template; [c] n.a. = not available; [d] in kJ/mol; [e] propagated uncertainties reflect 95% confidence intervals.

Imprinting factors of benzotriazoles were highest for the template molecule 1*H*-BT and decreased in the order 1*H*-BT > 5-$CH_3$-BT > 5-,6-$(CH_3)_2$-BT > 1-$CH_3$-BT. The observed sequence agrees with the notion that *IF* are highest for the template used for synthesis.[48] We verified this outcome by assessing *IF* of the same analytes on another custom-made MIP, where 5-,6-$(CH_3)_2$-BT was employed as a template instead of 1*H*-BT. The $IF_{(CH_3)_2-BT}$-values are shown in Table 1 for the 5-,6-$(CH_3)_2$-BT-imprinted MIP and they are of similar magnitude as *IF*-values for 1*H*-BT imprinted polymers. $IF_{(CH_3)_2-BT}$ decrease in the sequence 5-,6-$(CH_3)_2$-BT > 5-$CH_3$-BT > 1*H*-BT > 1-$CH_3$-BT confirming that the selectivity was highest for the template molecule. With both MIPs, we did not observe selective interactions of 1-$CH_3$-BT. Absence of selectivity for *N*-substituted benzotriazole suggests that the interactions of analytes with the polymer was based on hydrogen bonding of the triazole moiety with the carboxylic acid functional group of the monomer (methacrylic acid, Figure 3). Substitution at the 1*H* position on the triazole ring caused complete loss of selectivity towards 1-$(CH_3)$-BT on both polymers.

Further evidence for the selectivity of the MIPs was obtained from the comparisons of the apparent interaction enthalpies, $\Delta H_{MIP}$,[63] with various analytes, and interaction enthalpies of non-imprinted polymers, $\Delta H_{NIP}$ (Table 1). $\Delta H_{MIP}$ were most negative, that is most favourable, for the template molecule 1*H*-BT and became less negative for the substituted benzotriazoles. $\Delta H_{MIP}$-values ranged between 7.0 and 16 kJ/mol which is in the lower range of interaction enthalpies for hydrogen bonding (8-84 kJ/mol,[64,65]). Note that interactions of benzotriazoles with non-imprinted materials were also exothermic but the difference between MIP and NIP, $\Delta H_{MIP} - \Delta H_{NIP}$, revealed the larger selectivity of the MIPs. $\Delta H_{MIP} - \Delta H_{NIP}$ for benzotriazoles followed the same sequence reported for *IF*-values. However, values approached zero for the remaining compounds showing the lack of selective interactions of the MIP with benzothiazole, naphthalene, and atrazine.

## Isotope fractionation from incomplete analyte extraction

We quantified the extent of C and N isotope fractionation from analyte-MIP interactions in a separate experiment on MISPE cleanup step **E** (Figure 1). Table 2 shows mass fractions, $m_i$,

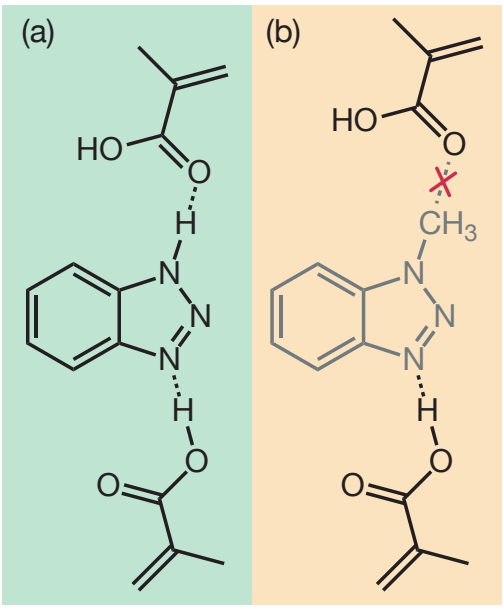


**Figure 3.** (a) Hydrogen bonding between the template, 1*H*-BT, and the functional monomer, methacrylic acid, used for imprinting enables selective interactions. (b) Absence of selective binding due to *N*-methyl substitution in 1-$CH_3$-BT.

and the corresponding $\delta^{13}$C and $\delta^{15}$N-values of 1*H*-BT recovered in three sample fractions ($F_i$). The total 1*H*-BT recovery was 99%. $F_1$ corresponds to the fraction of analyte collected after breakthrough during the loading of the cartridge with 1*H*-BT in dichloromethane. This fraction amounted to 41% of the total analyte mass. $F_2$ is the fraction of analyte obtained through washing of the cartridge with the identical solvent (42%). $F_3$ reflects the remaining 16% of 1*H*-BT that were recovered from the MIP through elution with methanol. The same type of experiment was carried out with dichloromethane extracts of river water using five-fold higher MIP (500 mg). As a consequence of higher retention capacity, no 1*H*-BT was detected in $F_1$, whereas all 1*H*-BT mass was recovered in the two remaining fractions, $F_2$ (74%, Table 2) and $F_3$ (26%).

The C isotope signatures of 1*H*-BT in the presence and absence of organic matrix from river water samples varied only slightly (±1‰) in the three fractions. The extent of C isotope fractionation pertinent to the MISPE cleanup step calculated with eq. 4, $\Delta^{13}$C, was negligible regardless of the sample matrix (−0.6 ± 1.4‰ and 0.1 ± 1.1‰, Table 2). By contrast, $\delta^{15}$N values of 1*H*-BT varied substantially (up to 13‰) between the three sample fractions $F_1$ to $F_3$. Due to the almost complete recovery of the analyte after the elution with methanol, MISPE induced N isotope fractionation,

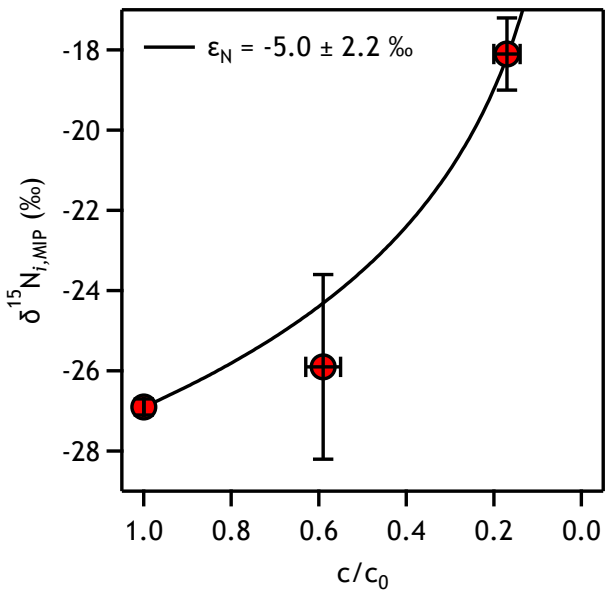


**Figure 4.** N isotope fractionation of $1H$-BT through stepwise elution from the MIP. $\delta^{15}N_{iMIP}$ ($\pm 1\sigma$) stand for the calculated N isotope signatures of $1H$-BT remaining on the MIP after elution of different $1H$-BT fractions. $c/c_0$ is the fraction of $1H$-BT remaining associated with the MIP. The data was generated by using information from Table 2 and eqs. 6 and 7. The solid line was obtained through non-linear regression of eq. 5 with an $\epsilon_N$ of $-5.0 \pm 2.2‰$.

$\Delta^{15}N$ is, nevertheless, negligible within uncertainty in both sample matrices ($-1.4 \pm 1.3‰$ and $-0.2 \pm 1.1‰$).

These observations suggests that a non-stoichiometric recovery of the analyte after the MISPE cleanup step would not cause systematic C isotope fractionation whereas N isotope signatures could be biassed towards more positive $\delta^{15}N$ values. We tentatively quantified an operational N isotope enrichment factor, $\epsilon_N$, from the small data set for the MISPE cleanup step **E** in absence of organic matrix using eq. 5. Figure 4 shows the average N isotope signatures of $1H$-BT that remained associated with the MIP ($\delta^{15}N_{i,MIP}$, eq. 7) after sequential loading step $F_1$ and $F_2$, respectively (blue and green areas). The most enriched fraction of $1H$-BT, $F_3$, with a $\delta^{15}N$ of $-18.1 \pm 0.9‰$, was eluted from the MIP through the change of solvent (red area in Figure 3). The N isotope fractionation trend was quantified with an $\epsilon_N$ of $-5.0 \pm 2.2‰$ (eq. 5) and illustrates that the $^{15}N$-containing $1H$-BT is retained preferentially by the MIP. This isotopic preference corresponds to an apparent $^{15}N$ kinetic isotope effect of $1.0054 \pm 0.0022$ (eq. 8) under the chosen experimental

**Table 2.** Sample fractions of $1H$-BT, $F_i$ collected during the MISPE cleanup step **E** (Figure 1): mass fractions of $1H$-BT, $m_i$, C and N isotope signatures, $\delta^{13}$C and $\delta^{15}$N, and extent of C and N isotope fractionation, $\Delta^{13}$C and $\Delta^{15}$N derived with eq. 4. [a]

| | | **reference** | **no matrix** | | | **river water extract** | | |
|---|---|---|---|---|---|---|---|---|
| $F_i$ | | | $F_1$ | $F_2$ | $F_3$ | $F_1$ | $F_2$ | $F_3$ |
| $m_i$ | (-) [b] | 1.00 ± 0.03 | 0.41 ± 0.02 | 0.42 ± 0.02 | 0.16 ± 0.03 | n.d | 0.74 ± 0.02 | 0.26 ± 0.02 |
| $\delta^{13}$C | (‰) [b] | −26.1 ± 0.5 | −25.4 ± 0.3 | −25.8 ± 0.4 | −24.9 ± 0.1 | n.d. | −26.4 ± 0.2 | −25.6 ± 0.6 |
| $\delta^{15}$N | (‰) [b] | −26.9 ± 0.2 | −28.3 ± 0.1 | −25.6 ± 0.2 | −18.1 ± 0.9 | n.d. | −30.5 ± 0.3 | −17.5 ± 0.6 |
| $\Delta^{13}$C | (‰) [c] | 0.0 ± 1.3 | | −0.6 ± 1.4 | | | 0.1 ± 1.1 | |
| $\Delta^{15}$N | (‰) [c] | 0.0 ± 1.2 | | −1.4 ± 1.3 | | | −0.2 ± 1.1 | |

[a] Data for $F_1$ and $F_2$ determined from $1H$-BT in dichloromethane, $F_3$ in methanol, n.d. = not detected due to larger MIP mass used in MISPE cleanup step; [b] uncertainties are $\pm 1\sigma$ of triplicate measurements of concentrations or isotope ratios; [c] propagated uncertainties (95% confidence intervals).

conditions. The observation of N isotope fractionation in the absence of any isotope fractionation for C implies that the N atoms of 1*H*-BT were involved in the interactions with the MIP and confirms the above conclusion that the selectivity of the MIP is indeed based on H-bonding with the triazole moiety of the analyte (Figure 3). Finally, this $^{15}$N isotope effect implies that 1*H*-BT recoveries during the MISPE cleanup step of $\geq 81\%$ are sufficient to limit such shifts of $\delta^{15}$N to $\leq 1.1‰$ (eq. 9), that is to the typical precision of N isotope ratio measurements by GC/C/IRMS.[5]

## Application in wastewater treatment plants

We applied the sample preparation procedures shown in Figure 1 to determine the C and N isotope signatures of 1*H*-BT in the influent and effluent of a WWTP, one of the frequently encountered matrices of the pollutant with DOC contents of several mg C/L.[51,52] The outcome was verified through a comparison the $\delta^{13}$C and $\delta^{15}$N values with those from 1*H*-BT in dishwashing detergents sold in villages that discharge their sewer into the studied WWTP.

Figure 5 shows the $\delta^{13}$C and $\delta^{15}$N values of 1*H*-BT in the influent and effluent of the WWTP as well as in dishwashing detergents sold by retailers in the study area. $\delta^{13}$C and $\delta^{15}$N values of 1*H*-BT in dishwashing detergents span from $-27‰$ to $-23‰$ and $-11‰$ to $1‰$, respecitvely. $\delta^{13}$C cover a similar range observed previously by Spahr et al.[55] with a simplified approach whereas our analysis reveals an even wider distribution of $\delta^{15}$N in 1*H*-BT. The wastewater samples (**2** in Figure 1) contained substantial amounts of DOC that amounted to 7.3 and 28 mg C/L for effluent and influent, respectively. The substantial interferences on C isotope ratio measurements were reduced through an additional liquid-liquid extraction during step **F** (Figure 1). $\delta^{15}$N values of 1*H*-BT in influent and effluent samples were identical within uncertainty ($-4.5 \pm 0.9‰$ vs. $-5.6 \pm 1.3‰$) whereas the difference of their $\delta^{13}$C was only minimal ($-26.8 \pm 0.2‰$ vs. $-26.1 \pm 0.4‰$). Even though a quantitative analysis of the C and N isotope signatures in the WWTP and in dishwashing detergents is beyond the scope of this work, data in Figure 5 reveals some consistent trends which confirm the applicability of MISPE-based procedures for CSIA. Similar C and N isotope signatures of 1*H*-BT in influent and effluent agree with the frequently made observation that this micropollutant is not

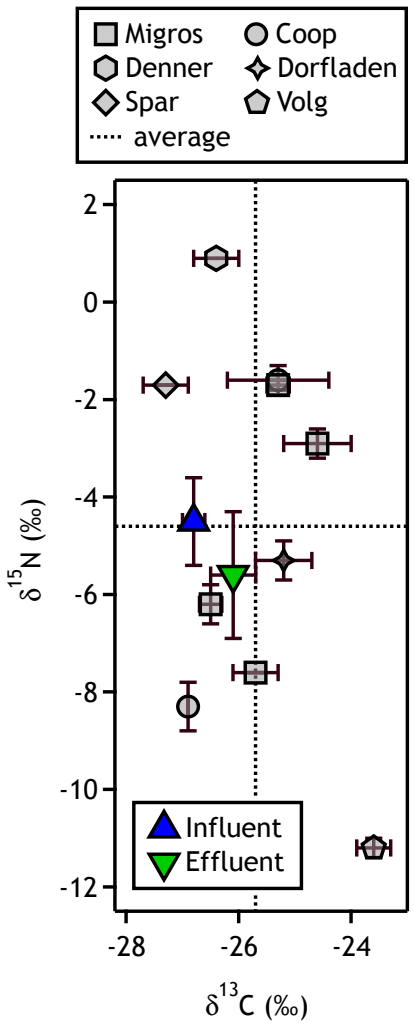


**Figure 5.** C and N isotope signatures of $1H$-BT in the influent and effluent of a WWTP (coloured triangles) as well as in various solid, liquid, and gel-like dishwashing detergents sold by retailers in the study area (grey symbols). The dashed lines correspond to the arithmetic mean of $\delta^{13}$C and $\delta^{15}$N of $1H$-BT in detergent samples. Error bars represent $\pm 1\sigma$. $1H$-BT influent and effluent concentrations were 4.3 and 3.8 $\mu$g/L, respectively.

degraded during the waste water treatment process.[51,52] Moreover, those values are also within the range of $\delta^{13}$C and $\delta^{15}$N values found in dishwashing detergents that are sold in the study area and they are within less than $1‰$ of their average values.

# Conclusion

Our work illustrates that sample treatment procedures which rely on the selective cleanup of enriched organic micropollutants by molecularly-imprinted polymer offer new perspectives for CSIA. Extractions of organic micropollutants in large volume samples by conventional SPE are an essential step to enrich adequate amounts of analytes for isotope-ratio mass spectrometry but they will inevitably lead to concomitant enrichment of organic matter. This matrix can be removed selectively in organic extracts with MIPs. The application of molecularly-imprinted polymers for CSIA of 1*H*-BT especially in influent and effluent samples from WWTPs revealed, however, that despite good selectivity, organic matrix interferences may become too large thus making the application of MISPE impracticable. Our analysis suggest that the C-normalized concentration ratio of dissolved organic carbon (DOC) to micropollutant can be a useful parameter to assess the feasibility of MISPE-based sample cleanup for CSIA, particularly for measurements of C isotope ratios. In fact, the C-normalized DOC:1*H*-BT ratio decreased systematically as a consequence of the series of treatment of WWTP samples. Whereas the DOC:1*H*-BT ratio in the aqueous WWTP influent was 11000 (**1** in Figure 1), it decreased to 860 in sample **3** after SPE and 340 in sample **5** after MISPE. In WWTP effluent, the DOC:1*H*-BT ratio decreased from 3200 in the aqueous effluent (**1**) to 190 after SPE (**3**) and 76 (**5**) after MISPE. Whereas we implemented liquid-liquid extraction in order to further reduce DOC:1*H*-BT ratios in WWTP samples, alternative approaches such as preparative HPLC on sample **5** could also be applied.[39] A systematic and quantitative assessment of the acceptable ratio of matrix:micropollutant is warranted to assess the feasibility of MISPE sample preparation for CSIA more generally. Such efforts will enable the application of stable isotope analyses for tracking sources and transformation processes of many contaminants of emerging concerns including, for example, pharmaceuticals, pesticides, and water disinfection byproducts.[11,12,16,17,39]

## Acknowledgement

This work was supported by the Swiss National Science Foundation (grant no. CRSII2-141805). We thank Stefanie Jucker, Hans-Jürgen Schindler, Samuel Derrer, Marius Wiesmann, Alessandra Sodero, Tony Merle, and Aileen Melsbach for experimental support.

## Supporting Information Available

Description of field site and sampling campaign, additional preparation steps for dishwashing detergents, derivation of interaction enthalpies, molecular structure of analytes. This material is available free of charge via the Internet at `http://pubs.acs.org/`.

## References

(1) Elsner, M.; Imfeld, G. *Curr. Opin. Biotech.* **2016**, *41*, 60–72.

(2) Hofstetter, T. B.; Berg, M. *TrAC-Trends Anal. Chem.* **2011**, *30*, 618 – 627.

(3) Hofstetter, T. B.; Bolotin, J.; Pati, S. G.; Skarpeli-Liati, M.; Spahr, S.; Wijker, R. S. *CHIMIA* **2014**, *68*, 788–792.

(4) Schmidt, T. C.; Jochmann, M. A. *Annu. Rev. Anal. Chem.* **2012**, *5*, 133–155.

(5) Elsner, M.; Jochmann, M.; Hofstetter, T.; Hunkeler, D.; Bernstein, A.; Schmidt, T.; Schimmelmann, A. *Anal. Bioanal. Chem.* **2012**, *403*, 2471–2491.

(6) Hofstetter, T. B.; Schwarzenbach, R. P.; Bernasconi, S. M. *Environ. Sci. Technol.* **2008**, *42*, 7737–7743.

(7) Thullner, M.; Centler, F.; Richnow, H. H.; Fischer, A. *Org. Geochem.* **2012**, *42*, 1440 – 1460.

(8) Ivdra, N.; Fischer, A.; Herrero-Martín, S.; Giunta, T.; Bonifacie, M.; Richnow, H.-H. *Environ. Sci. Technol.* **2016**, *51*, 446–454.

(9) Gilevska, T.; Gehre, M.; Richnow, H.-H. *Journal of Pharmaceutical and Biomedical Analysis* **2015**, *115*, 410–417.

(10) Kaown, D.; Shouakar-Stash, O.; Yang, J.; Hyun, Y.; Lee, K.-K. *Ground Water* **2014**, *52*, 875–885.

(11) Spahr, S.; Bolotin, J.; Schleucher, J.; Ehlers, I.; von Gunten, U.; Hofstetter, T. B. *Anal. Chem.* **2015**, *87*, 2916–2924.

(12) Spahr, S.; von Gunten, U.; Hofstetter, T. B. *Environ. Sci. Technol.* **2017**, *51*, 13170–13179.

(13) Arnold, W. A.; Bolotin, J.; von Gunten, U.; Hofstetter, T. B. *Environ. Sci. Technol.* **2008**, *42*, 7778–7785.

(14) Hunkeler, D.; Laier, T.; Breider, F.; Jacobsen, O. S. *Environ. Sci. Technol.* **2012**, *46*, 6096–6101.

(15) Wijker, R. S.; Bolotin, J.; Nishino, S. F.; Spain, J. C.; Hofstetter, T. B. *Environ. Sci. Technol.* **2013**, *47*, 6872–6883.

(16) Maier, M. P.; Prasse, C.; Pati, S. G.; Nitsche, S.; Li, Z.; Radke, M.; Meyer, A. H.; Hofstetter, T. B.; Ternes, T. A.; Elsner, M. *Environ. Sci. Technol.* **2016**, *50*, 10933–10942.

(17) Schürner, H. K. V.; Maier, M. P.; Eckert, D.; Brejcha, R.; Neumann, C.-C.; Stumpp, C.; Cirpka, O. A.; Elsner, M. *Environ. Sci. Technol.* **2016**, *50*, 5729–5739.

(18) Badin, A.; Broholm, M. M.; Jacobsen, C. S.; Palau, J.; Dennis, P.; Hunkeler, D. *J. Contam. Hydrol.* **2016**, *192*, 1–19.

(19) Rosell, M.; Gonzalez-Olmos, R.; Rohwerder, T.; Rusevova, K.; Georgi, A.; Kopinke, F.-D.; Richnow, H.-H. *Environ. Sci. Technol.* **2012**, *46*, 4757–4766.

(20) Ratti, M.; Canonica, S.; McNeill, K.; Bolotin, J.; Hofstetter, T. B. *Environ. Sci. Technol.* **2015**, *49*, 9797–9806.

(21) Ratti, M.; Canonica, S.; McNeill, K.; Bolotin, J.; Hofstetter, T. B. *Environ. Sci. Technol.* **2015**, *49*, 12766–12773.

(22) Merritt, D. A.; Hayes, J. M. *Anal. Chem.* **1994**, *66*, 2336–2347.

(23) Krummen, M.; Hilkert, A. W.; Juchelka, D.; Duhr, A.; Schlüter, H.-J.; Pesch, R. *Rapid Commun. Mass Spectrom.* **2004**, *18*, 2260–2266.

(24) Sessions, A. L. *J. Sep. Sci.* **2006**, *29*, 1946–61.

(25) Gilevska, T.; Gehre, M.; Richnow, H.-H. *Anal. Chem.* **2014**, *86*, 7252–7257.

(26) Passeport, E.; Landis, R.; Mundle, S. O. C.; Chu, K.; Mack, E. E.; Lutz, E. J.; Sherwood Lollar, B. *Environ. Sci. Technol.* **2014**, *48*, 9582–9590.

(27) Aelion, M. C.; Höhener, P.; Hunkeler, D.; Aravena, R. *Environmental Isotopes in Biodegradation and Bioremediation*; CRC Press: Boca Raton, 2010.

(28) Jochmann, M. A.; Schmidt, T. C. *Compound-specific Stable Isotope Analysis*; The Royal Society of Chemistry, 2012.

(29) Horst, A.; Renpenning, J.; Richnow, H.-H.; Gehre, M. *Anal. Chem.* **2017**, *89*, 9131–9138.

(30) Heckel, B.; Rodríguez-Fernández, D.; Torrentó, C.; Meyer, A. H.; Palau, J.; Domènech, C.; Rosell, M.; Soler, A.; Hunkeler, D.; Elsner, M. *Anal. Chem.* **2017**, *89*, 3411–3420.

(31) Renpenning, J.; Kümmel, S.; Hitzfeld, K. L.; Schimmelmann, A.; Gehre, M. *Anal. Chem.* **2015**, *87*, 9443–9450.

(32) Horst, A.; Lacrampe-Couloume, G.; Sherwood Lollar, B. *Anal. Chem.* **2015**, *87*, 10498–10504.

(33) Berg, M.; Bolotin, J.; Hofstetter, T. B. *Anal. Chem.* **2007**, *79*, 2386–93.

(34) Skarpeli-Liati, M.; Turgeon, A.; Garr, A. N.; Arnold, W. A.; Cramer, C. J.; Hofstetter, T. B. *Anal. Chem.* **2011**, *83*, 1641–1648.

(35) Zwank, L.; Berg, M.; Schmidt, T. C.; Haderlein, S. B. *Anal. Chem.* **2003**, *75*, 5575–5583.

(36) Passeport, E.; Landis, R.; Lacrampe-Couloume, G.; Lutz, E. J.; Mack, E. E.; West, K.; Morgan, S.; Sherwood Lollar, B. *Environ. Sci. Technol.* **2016**, *50*, 12197–12204.

(37) Herrero-Martín, S.; Nijenhuis, I.; Richnow, H.-H.; Gehre, M. *Anal. Chem.* **2015**, *87*, 951–959.

(38) Schwarzenbach, R. P.; Escher, B. I.; Fenner, K.; Hofstetter, T. B.; Johnson, C. A.; von Gunten, U.; Wehrli, B. *Science* **2006**, *313*, 1072–7.

(39) Schreglmann, K.; Hoeche, M.; Steinbeiss, S.; Reinnicke, S.; Elsner, M. *Anal. Bioanal. Chem.* **2013**, *405*, 2857–2867.

(40) Martín-Esteban, A. *TrAC Trends Anal. Chem.* **2013**, *45*, 169–181.

(41) Sellergren, B. *TrAC Trends Anal. Chem.* **1999**, *18*, 164–174.

(42) Sellergren, B. *TrAC Trends Anal. Chem.* **1997**, *16*, 310–320.

(43) Sellergren, B. *Angew. Chem. Int. Ed.* **2000**, *39*, 1031–1037.

(44) Turiel, E.; Martín-Esteban, A. *Anal. Chim. Acta* **2010**, *668*, 87–99.

(45) Komiyama, M.; Takeuchi, T.; Mukawa, T.; Asanuma, H. *Molecular Imprinting: From Fundamentals to Applications*; Wiley-VCH Verlag GmbH & Co. KGaA, 2004.

(46) Sun, Z.; Schuessler, W.; Sengl, M.; Niessner, R.; Knopp, D. *Anal. Chim. Acta* **2008**, *620*, 73–81.

(47) Stevenson, D. *TrAC Trends Anal. Chem.* **1999**, *18*, 154–158.

(48) Caro, E.; Marcé, R. M.; Borrull, F.; Cormack, P.; Sherrington, D. *TrAC Trends Anal. Chem.* **2006**, *25*, 143–154.

(49) Huntscha, S.; Singer, H. P.; McArdell, C. S.; Frank, C. E.; Hollender, J. *J. Chromatogr. A* **2012**, *1268*, 74–83.

(50) Hollender, J.; Zimmermann-Steffens, S. G.; Koepke, S.; Krauss, M.; McArdell, C. S.; Ort, C.; Singer, H. P.; von Gunten, U.; Siegrist, H. *Environ. Sci. Technol.* **2009**, *43*, 7862–7869.

(51) Schymanski, E. L.; Singer, H. P.; Longrée, P.; Loos, M.; Ruff, M.; Stravs, M. A.; Ripollés Vidal, C.; Hollender, J. *Environ. Sci. Technol.* **2014**, *48*, 1811–1818.

(52) Huntscha, S.; Hofstetter, T. B.; Schymanski, E. L.; Spahr, S.; Hollender, J. *Environ. Sci. Technol.* **2014**, *48*, 4435–4443.

(53) Chapuis, F.; Pichon, V.; Lanza, F.; Sellergren, B.; Hennion, M. C. *J Chromatogr B* **2004**, *804*, 93–101.

(54) Canonica, S.; Meunier, L.; von Gunten, U. *Water Res.* **2008**, *42*, 121–128.

(55) Spahr, S.; Huntscha, S.; Bolotin, J.; Maier, M. P.; Elsner, M.; Hollender, J.; Hofstetter, T. B. *Anal. Bioanal. Chem.* **2013**, *405*, 2843–2856.

(56) Schimmelmann, A.; Lewan, M. D.; Wintsch, R. P. *Geochim. Cosmochim. Acta* **1999**, *63*, 3751–3766.

(57) Schimmelmann, A.; Albertino, A.; Sauer, P. E.; Qi, H.; Molinie, R.; Mesnard, F. *Rapid Commun. Mass Spectrom.* **2009**, *23*, 3513–3521.

(58) Pati, S. G.; Kohler, H.-P. E.; Hofstetter, T. B. In *Measurement and Analysis of Kinetic Isotope Effects*; Harris, M. E., Anderson, V. E., Eds.; Academic Press, 2017; pp 292–329.

(59) Meier-Augenstein, W. *J Chromatogr A* **1999**, *842*, 351–371.

(60) Ricci, M. P.; Merritt, D. A.; Freeman, K. H.; Hayes, J. M. *Organic Geochemistry* **1994**, *21*, 561–571.

(61) Sherwood Lollar, B.; Hirschorn, S. K.; Chartrand, M. M. G.; Lacrampe-Couloume, G. *Anal. Chem.* **2007**, *79*, 3469–3475.

(62) Matsui, J.; Miyoshi, Y.; Doblhoff-Dier, O.; Takeuchi, T. *Anal. Chem.* **1995**, *67*, 4404–4408.

(63) Sellergren, B.; Shea, K. J. *J. Chromatogr. A* **1995**, *690*, 29–39.

(64) Laurence, C.; Berthelot, M. *Perspectives in Drug Discovery and Design* **2000**, *18*, 39–60.

(65) Yilmaz, E.; Schmidt, R. H.; Mosbach, K. In *Molecularly Imprinted Materials*; Yan, M., Ramström, O., Eds.; CRC Press, 2004; pp 25–57.

# TOC art

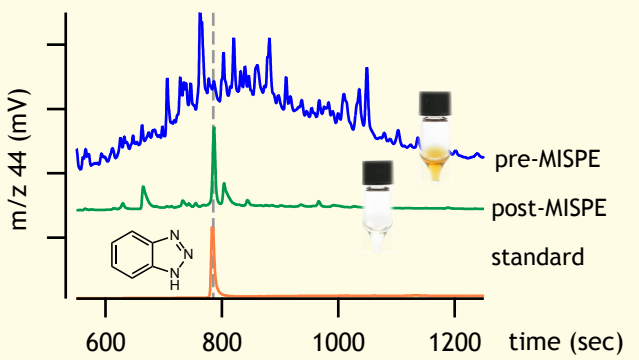
m/z 44 (mV)
pre-MISPE
post-MISPE
standard
600
800
1000
1200
time (sec)